ENGINEERING TRANSACTIONS • *Engng. Trans.* • **47**, 2, 183–201, 1999
Polish Academy of Sciences • Institute of Fundamental Technological Research
10.24423/engtrans.628.1999

MASS MINIMIZATION OF DYNAMICALLY LOADED MACHINE FOUNDATIONS USING DIFFERENT SUBSOIL MODELS

Z. SIENKIEWICZ and B. WILCZYŃSKI

TECHNICAL UNIVERSITY OF KOSZALIN
ul. Racławicka 15/17, Koszalin, Poland
email: sien@lew.tu.koszalin.pl bwil@lew.tu.koszalin.pl

The effect of variation of the shear wave velocity profile of a layered soil on a minimal mass of a rigid machine foundation under behavior constraints on vibration and normal stress contact amplitudes and side constraints is numerically studied. The nonlinear programming problem has been solved by an iterative application of a sequential linear programming. The dynamic response of the machine foundation to unbalanced forces is evaluated including the dynamic soil-block interaction. The mixed-boundary value problem of elastodynamics was formulated as the system of Fredholm integral equations of the first kind with the Green's functions for a half-space as kernels and contact tractions as unknowns. The solution of the integral equations was accomplished numerically by a Boundary Element Method. In addition, the effect of embedment of the block into the soil was included by means of a local dynamic boundary used to simulate the backfill. Numerical results illustrate the sensitivity of the optimum design with respect to variations in problem preassigned parameters.

1. INTRODUCTION

Reciprocating machines are frequently encountered in practice and they are usually mounted on rigid-type reinforced concrete blocks, [1, 2]. The machine foundations transmit the dynamic loads to the supporting soil and its vibrations are due to dynamic deformations of the soil medium. In the modern advanced analysis, the dynamic properties of the inertial supporting medium are described by means of the complex-valued impedance functions, [3, 4, 5]. To find the functions, a mixed boundary-value problem must be solved, in which displacements are prescribed at the contact area between the foundation and the soil, and tractions vanish at the free surface of the soil. In addition, the radiation conditions at infinity must be satisfied. Given the impedance functions of the soil and geometrical and inertial properties of the machine-block system, it is possible to calculate the dynamic response of the machine foundation to unba-

lanced forces. The operational requirements of the machine limit the amplitudes of foundation vibration to small values. Furthermore, in practice some additional structural and psychological criteria should be fulfilled because the wave energy transmitted through the underlying soil from the vibration foundation must not cause harmful effects on other precision equipments or machines and adjoining structures and should not be annoying to persons standing close to the vibrating machinery. Generally, the design of a machine foundation is a trial-and-error procedure that should lead to a safe and economical foundation block satisfying the design criteria, [1, 2]. The engineering decision-making process may be helped by integrating the dynamic analysis model with the optimization procedure, [6, 7]. It leads to the rational design of a dynamically loaded machine foundation that is the best of all possible designs within a prescribed objective and a given set of behavior constraints. This approach was developed by the authors in the papers [8 – 11]. The objective of this investigation is to evaluate the influence of the nature of soil profile on the optimal mass of massive rigid rectangular foundation.

Generally, natural cohesionless as well as cohesive soil deposits increase in rigidity with depth as a reflection of the increase in overburden pressure. The increase may be continuous or discontinuous as in the case of layered system, and it is influenced by the void ratio, the level of effective confining pressure, the intrinsic characteristics (e.g. grain shape and size distribution, mineralogical composition), the degree of saturation, vibration history and others. A typical case is the presence of a stiffer material at a relatively shallow depth. The dynamic response of a machine foundation on a soil stratum underlain by a stiffer medium can be substantially different from the response of an identical foundation on a uniform half-space. Thus it is imperative to study the sensitivity of the optimal design of the machine foundation with respect to variations in parameters defining such soil deposits, [12]. In this paper two types of idealized soil profiles under the base of foundation block are considered: (1) uniform layer overlying a uniform half-space (shear wave velocity is constant in the layer and the underlying half-space with finite jump between them), and (2) layer with linearly varying elastic properties overlying a uniform half-space (shear wave velocity is linearly varying in the layer under the base being constant in the underlying half-space). The assumed shear wave velocity profiles idealized in a rational way the variations of the shear wave velocity with depth in real sites as found by measurements.

2. Statement of the problem

Reinforced concrete block resting on the soil medium is dynamically loaded by unbalanced forces of a reciprocating machine (Fig. 1).

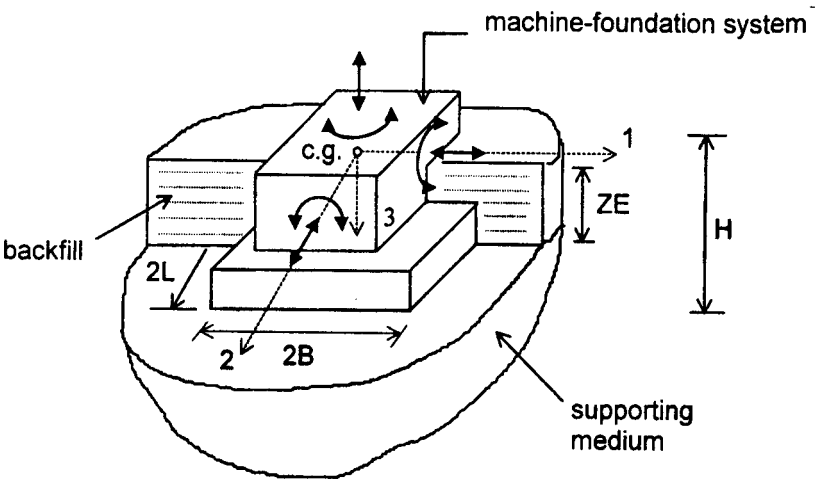

FIG. 1. Machine-foundation-soil system.

The problem of optimum design of vibrating 3-D machine foundation coupled to a half-space is a standard nonlinear programming problem and can be stated as (see Box. 1.):

BOX 1. Problem formulation

Find the vector of design variables $\mathbf{D}$ (dimensions of block) such that
$W(\mathbf{D})$ – weight (mass) of the concrete block $\rightarrow$ min
subject to behaviour constraints:

- on vibration amplitudes $\quad \mathbf{q}_{\max} \leqslant \mathbf{q}_{\text{feas}}$
- on amplitudes of contact stresses $\quad \sigma \leqslant \sigma_{\text{feas}}$
  and side constraints $\quad \mathbf{D}_{\text{l}} \leqslant \mathbf{D} \leqslant \mathbf{D}_{\text{u}},$

where: $\mathbf{D}_{\text{l}}$ and $\mathbf{D}_{\text{u}}$ are the lower and upper limiting values of a vector $\mathbf{D}$, and symbols with index feas mean allowable values of behaviour constraints.

3. RESPONSE ANALYSIS IN THE FREQUENCY DOMAIN

Consider a linearly elastic soil medium to occupy a region $V \cup V_B \in R^3$. Within this region we identify a half-space subregion V below the base of the block to represent the soil in its natural state, and a sublayer V_B to represent the disturbed soil (backfill) surrounding the block. The rigid body representing the machine-block system occupies an open, bounded region $V^* \in R^3$ and we choose

an inertial reference frame, $\{\mathbf{e}_1, \mathbf{e}_2, \mathbf{e}_3\}$ so that the centre of mass of the body is located at the origin

$$\int_{V^*} \rho_{\text{ref}} \mathbf{X} d\Omega = \mathbf{0} \tag{3.1}$$

where ρ_{ref} is the density of the rigid body in the reference placement V^* and $\mathbf{X}$ denotes the initial position vector of a particle, measured from the origin of the inertial reference frame. We also attach at the centre of mass a set of nonparallel, noncoplanar unit vectors $\{\mathbf{b}_1(t), \mathbf{b}_2(t), \mathbf{b}_3(t)\}$ fixed in V^*. This time-dependent set of vectors is called the body frame since they move with the body. It is assumed that at time $t = 0$, the body frame is parallel to the inertial frame. The perfect bonding exists between the half-space V and the rigid body along the contact surface S_C^N and between the sublayer V_B and the body along the contact surface S_C^B. It is assumed however, that at the horizontal interface S_C^{N-B} between the half-space and the sublayer, the condition of continuity of displacements is not satisfied and that the surfaces of the separated regions are free of tractions. Then the tractions at the base of the rigid body are equal to those of the body placed on the soil surface, while the backfill reactions are to be evaluated independently by a local modelling. It should be noted that the local approach to modelling of the embedment effects is supported by experimental investigations leading to reasonable agreement between the theory and experiment, [13]. Denoting the Fourier transform of time function $f(t)$ by $\hat{f}(\omega)$, the linearized equations of motion for the idealized machine-block system in body frame can be written in the frequency domain as

$$-\omega^2 \mathbf{M} \hat{\mathbf{U}}(\omega) = \hat{\mathbf{P}}(\omega) + \hat{\mathbf{P}}_S(\omega), \tag{3.2}$$

in which ω is the excitation frequency, $\hat{\mathbf{U}}(\omega)$ is the Fourier transform of the displacement vector, $\hat{\mathbf{P}}(\omega)$ is the Fourier transform of the load vector, $\hat{\mathbf{P}}_S(\omega)$ is the Fourier transform of the interaction force vector, and $\mathbf{M}$ is the inertia matrix. The generalized displacement vector $\hat{\mathbf{U}}(\omega)$ involves

$$\hat{\mathbf{U}}(\omega) = \left\{\hat{\Delta}_1(\omega), \hat{\Delta}_2(\omega), \hat{\Delta}_3(\omega), \hat{\Theta}_1(\omega), \hat{\Theta}_2(\omega), \hat{\Theta}_3(\omega)\right\}, \tag{3.3}$$

where $(\hat{\Delta}_1(\omega), \hat{\Delta}_2(\omega, \hat{\Delta}_3(\omega))$ are the translations of the centre of mass of the rigid body and $(\hat{\Theta}_1(\omega), \hat{\Theta}_2(\omega), \hat{\Theta}_3(\omega))$ are the rotations. The external excitation is represented by the vector

$$\hat{\mathbf{P}}(\omega) = \{\hat{P}_1(\omega), \hat{P}_2(\omega), \hat{P}_3(\omega), \hat{M}_1(\omega), \hat{M}_2(\omega), \hat{M}_3(\omega)\} \tag{3.4}$$

which includes the resultant force $(\hat{P}_1(\omega), \hat{P}_2(\omega), \hat{P}_3(\omega))$, and the resulting moment $(\hat{M}_1(\omega), \hat{M}_2(\omega), \hat{M}_3(\omega))$. The generalized force $\hat{\mathbf{P}}_S(\omega)$ that the soil exerts

on the block

$$\hat{\mathbf{P}}_S(\omega) = \{\hat{P}_1^S(\omega), \hat{P}_2^S(\omega), \hat{P}_3^S(\omega), \hat{M}_1^S(\omega), \hat{M}_2^S(\omega), \hat{M}_3^S(\omega)\} \tag{3.5}$$

includes the reaction force $(\hat{P}_1^S(\omega), \hat{P}_2^S(\omega), \hat{P}_3^S(\omega))$ and the reaction moment $(\hat{M}_1^S(\omega), \hat{M}_2^S(\omega), \hat{M}_3^S(\omega))$. It is found that

$$\hat{\mathbf{P}}_S(\omega) = \int_{S_C} \mathbf{R}^T(\mathbf{x})\hat{\mathbf{T}}^{\mathbf{n}^*}(\mathbf{x},\omega)dS(\mathbf{x}), \qquad \mathbf{x} \in S_C = S_C^N \cup S_C^B \tag{3.6}$$

in which the 3×1 vector $\hat{\mathbf{T}}^{\mathbf{n}^*}(\mathbf{x},\omega) = \{\hat{T}_1^{\mathbf{n}^*}(\mathbf{x},\omega), \hat{T}_2^{\mathbf{n}}(\mathbf{x},\omega), \hat{T}_3^{\mathbf{n}^*}(\mathbf{x},\omega)\}$ represents the traction that the soil exerts on the block through $S_C, \mathbf{n}^*$ is the unit normal vector pointing outwards of V^* and the 3×6 matrix $\mathbf{R}(\mathbf{x})$ is given by

$$\mathbf{R}(\mathbf{x}) \begin{bmatrix} 1 & 0 & 0 & 0 & x_3 & -x_2 \\ 0 & 1 & 0 & -x_3 & 0 & x_1 \\ 0 & 0 & 1 & x_2 & -x_1 & 0 \end{bmatrix}. \tag{3.7}$$

To determine the distribution of the traction $\hat{\mathbf{T}}^{\mathbf{n}^*}(\mathbf{x},\omega)$ on the contact surface S_C^N, the dynamic contact problem between the rigid body and the soil must be solved. The displacement field in the soil medium $\hat{\mathbf{u}}(\mathbf{x},\omega) = \{\hat{u}_1(\mathbf{x},\omega), \hat{u}_2(\mathbf{x},\omega), \hat{u}_3(\mathbf{x},\omega)\}$, $\mathbf{x} \in V$, must satisfy the Navier equations of motion, the condition of vanishing tractions on the free surface of the half-space and the radiation conditions at infinity, [14]. At the soil-body interface S_C^N, the displacement field must satisfy the rigid body displacement

$$\hat{\mathbf{u}}(\mathbf{x},\omega) = \mathbf{R}(\mathbf{x})\hat{\mathbf{U}}(\omega), \qquad \mathbf{x} \in S_C^N. \tag{3.8}$$

The displacements in the soil medium V due to the tractions $\hat{\mathbf{T}}^{\mathbf{n}}(\mathbf{x},\omega) = \{\hat{T}_1^{\mathbf{n}}(\mathbf{x},\omega), \hat{T}_2^{\mathbf{n}}(\mathbf{x},\omega), \hat{T}_3^{\mathbf{n}}(\mathbf{x},\omega)\}$, $\mathbf{x} \in S_C^N$, acting at the interface $\mathbf{x} \in S_C^N$, can be expressed in the form

$$\hat{\mathbf{u}}(\mathbf{x},\omega) = \int_{S_C^N} \hat{\mathbf{G}}(\mathbf{x},\mathbf{y},\omega)\hat{\mathbf{T}}^{\mathbf{n}}(\mathbf{y},\omega)dS(\mathbf{y}), \qquad \mathbf{x} \in V, \qquad \mathbf{y} \in S_C^N, \tag{3.9}$$

in which $\hat{\mathbf{G}}(\mathbf{x},\mathbf{y},\omega)$ is the 3×3 displacement Green's function matrix where the jth column corresponds to the displacement vector at $\mathbf{x}$ due to a unit harmonic force at $\mathbf{y}$ acting in the jth direction and $\mathbf{n}$ is the unit normal vector pointing outwards of V. An integral equation approach results from selecting the point $\mathbf{x}$ on the surface S_C^N. Assuming in Eq. (3.9) that the displacement vector $\hat{\mathbf{u}}(\mathbf{x},\omega)$ is known for $\mathbf{x} \in S_C^N$, from the rigid body motion (3.8) one gets

$$\mathbf{R}(\mathbf{x})\hat{\mathbf{U}}(\omega) = \int_{S_C^N} \hat{\mathbf{G}}(\mathbf{x},\mathbf{y},\omega)\hat{\mathbf{T}}^{\mathbf{n}}(\mathbf{y},\omega)dS(\mathbf{y}), \qquad \mathbf{x},\mathbf{y} \in S_C^N \tag{3.10}$$

which corresponds to a Fredholm integral equation of the first kind for the unknown traction $\hat{\mathbf{T}}^{\mathbf{n}}(\mathbf{n},\omega)$ on the contact surface S_C^N. Due to the linearity of the problem, the solution of Eq. (3.10) can be written in the form

$$\hat{\mathbf{T}}^{\mathbf{n}}(\mathbf{x},\omega) = \hat{\mathbf{H}}(\mathbf{x},\omega)\hat{\mathbf{U}}(\omega), \qquad \mathbf{x} \in S_C^N, \tag{3.11}$$

where $\hat{\mathbf{H}}(\mathbf{x},\omega)$ is the 3×6 matrix of contact tractions for unit rigid-body displacements corresponding to each of the six degrees of freedom of the rigid body. Similarly, the traction vector $\hat{\mathbf{T}}^{n}(\mathbf{x},\omega)$ on the contact surface S_C^B can be expressed in the form

$$\hat{\mathbf{T}}^{\mathbf{n}}(\mathbf{x},\omega) = \hat{\mathbf{H}}(\mathbf{x},\omega)\hat{\mathbf{U}}(\omega), \qquad \mathbf{x} \in S_C^B, \tag{3.12}$$

in which the matrix of contact tractions $\hat{\mathbf{H}}(\mathbf{x},\omega), \mathbf{x} \in S_C^B$, represents the effect of backfill and, due to the local modelling, it is assumed that the tractions at any point on the vertical side are related to the displacements only at the point where the reaction is considered. In this approach, the matrix $\hat{\mathbf{H}}(\mathbf{x},\omega)$, $\mathbf{x} \in S_C^B$, is easili obtained from an analytical solution of a dynamic contact problem between a rigid cylindrical inclusion and a soil medium under the cylindrical plane-strain condition, [15]. It is noted that $\mathbf{n} = -\mathbf{n}^*$ and $\hat{\mathbf{T}}^{\mathbf{n}}(\mathbf{x},\omega) = -\hat{\mathbf{T}}^{\mathbf{n}^*}(\mathbf{x})$. Then, substitution from (3.11) and (3.12) into (3.6) gives

$$\hat{\mathbf{P}}_S(\omega) = -\hat{\mathbf{K}}(\omega)\hat{\mathbf{U}}(\omega) \tag{3.13}$$

in which

$$\hat{\mathbf{K}}(\omega) = \int_{S_C} \mathbf{R}^T(\mathbf{x})\hat{\mathbf{H}}(\mathbf{x},\omega)dS(\mathbf{x}), \qquad \mathbf{x} \in S_C = S_C^N \cup S_C^B \tag{3.14}$$

is the 6×6 impedance matrix of the soil medium. Including the Eq. (3.13) in the equation of motion (3.2) leads to the following equation of motion of the block-soil system in the frequency domain:

$$(\hat{\mathbf{K}}(\omega) - \omega^2\mathbf{M})\hat{\mathbf{U}}(\omega) = \hat{\mathbf{P}}(\omega) \tag{3.15}$$

Let the machine-block-soil system posseses two orthogonal vertical planes of symmetry and let the body frame be directed along the principal body axes, then the inertia matrix is diagonal

$$\mathbf{M} = \mathrm{diag}\{m, m, m, J_{11}, J_{22}, J_{33}\}, \tag{3.16}$$

where m is the total mass of the machine and block, and J_{11}, J_{22} and J_{33} are the mass moment of inertia of the considered system with respect to the coordinate axes. The solution of Eq. (3.15) is given by

$$\hat{\mathbf{U}}(\omega) = (\hat{\mathbf{K}}(\omega) - \omega^2\mathbf{M})^{-1}\hat{\mathbf{P}}(\omega). \tag{3.17}$$

Finally, the U_j components of the steady-state motion of the machine-foundation system at the centre of mass are obtained from

$$U_j(t) = U_{0j}\exp[i(\omega t + \Xi_j)], \qquad j = 1, 2, , ..., 6, \tag{3.18}$$

where the real amplitudes of motion U_{0j} and the phase angles Ξ_j are given by

$$U_{0j} = \left(\left(\mathrm{Re}\hat{U}_j\right)^2 + \left(\mathrm{Im}\hat{U}_j\right)^2\right)^{\frac{1}{2}}, \Xi_j = \arctan\frac{\mathrm{Im}\hat{U}_j}{\mathrm{Re}\hat{U}_j}. \tag{3.19}$$

4. Optimization procedure

The optimization problem formulated in Box 1 is a standard nonlinear programming problem [16]. For efficient structural systems the approximate methods are widely used [17, 18]. To obtain a minimum mass of machine foundation dynamically interacting with soil, the sequential linear programming (SLP) is adopted [16, 19, 20]. Linear approximation of non-linear functions is accomplished by replacing the nonlinear functions of vibration amplitudes and subsoil stresses with their first-order Taylor series terms (Box. 2). Then this linearized problem is solved using Simplex algorithm [16]. The finite difference method is adopted to obtain the gradients of the objective function and behaviour constraints. In order to control the stability and convergence of the algorithm, a set of *move limits* is added to the constraints of the SLP problem [18, 20].

Box 2. Linearized optimization problem

$$\text{Min } W(\mathbf{D}) = W(\mathbf{D}^p) + < \nabla^T W(\mathbf{D}^p), \Delta\mathbf{D}^p > ,$$
$$\text{subject to: } g_j(\mathbf{D}) = g_j(\mathbf{D}^p) + < \nabla^T g_j(\mathbf{D}^p), \Delta\mathbf{D}^p > \leqslant g_{j\text{feas}} ,$$
$$\mathbf{D}_l \leqslant \mathbf{D} \leqslant \mathbf{D}_u ,$$
$$\Delta\mathbf{D}_l \leqslant \Delta\mathbf{D} \leqslant \Delta\mathbf{D}_u ,$$

where:
p is iteration number,
$g_j(\mathbf{D}) \equiv q_{j\max}(\mathbf{D})$, $g_j(\mathbf{D}) \equiv \sigma(\mathbf{D})$,
$\mathbf{D}^p$ is the design point about which linearization is performed,
$\Delta\mathbf{D}$ are design changes,
and $\Delta\mathbf{D}_l$ and $\Delta\mathbf{D}_u$ are constants that represent move limits on $\Delta\mathbf{D}$.

5. Numerical results

A rigid massive rectangular block $2B \times 2L (B \leqslant L)$ resting on an inhomogeneous soil with depth-dependent properties and excited by unbalanced vertical and

horizontal forces from a single-cylinder reciprocating engine is to be optimized. The supporting medium consists of an independent backfill layer surrounding the block to the height ZE and a horizontal layer of constant thickness HL bonded to an underlying half-space, Fig. 2. The backfill is characterized by the shear wave velocity $V_S^{(B)}$, Poisson's ratio ν_b, density ρ_b and hysteretic damping constants ζ_{bs} and ζ_{bp} for shear and compressional waves, respectively. The layer under the base of block is characterized by a distribution of shear wave velocity $V_S^{(L)}(z)$, Poisson's ratio ν_1, density ρ_1 and hysteretic damping constants ζ_{1s} and ζ_{1p} for shear and compressional waves, respectively. The underlying half-space is characterized by the shear wave velocity $V_S^{(H)}$, Poisson's ratio ν_2, density ρ_2 and hysteretic damping constants ζ_{2s} and ζ_{2p} for shear and compressional waves, respectively. Two depth distributions of shear wave velocity in the layer are considered: (I) constant shear wave velocity and (II) linearly varying shear wave velocity. It leads to two velocity-depth functions for the medium under the base of the foundation block that have been assumed in the paper. The first profile, appropriate for pronounced layering, is described by piecewise continuous step-step function of depth variable, and the second one is given in the form of continuous ramp-step function of depth variable, that corresponds to bounded nonhomogeneity with no pronounced layering, Fig. 2.

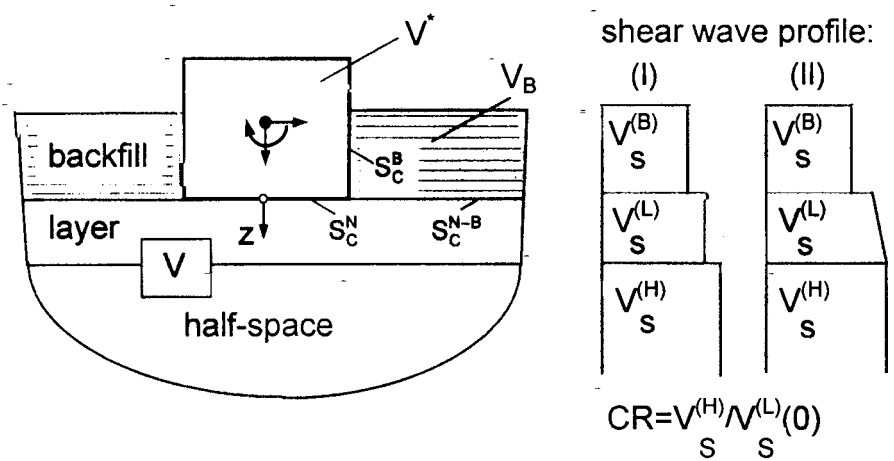

FIG. 2. Block-soil model and notation.

To determine the dynamic response of the machine-block system from Eqs. (3.17), (3.18) and (3.19), the impedance matrix of the soil medium $\hat{\mathbf{K}}(\omega)$ must be calculated. It is obtained from Eq. (3.14) if the 3×6 matrix of contact tractions $\hat{\mathbf{H}}(\mathbf{x}, \omega)$, $\mathbf{x} \in S_C$, is known. The solution of the integral Eq. (3.10) giving the matrix $\hat{\mathbf{H}}(\mathbf{x}, \omega)$, $\mathbf{x} \in S_C^N$, in accordance with the Eq. (3.11) is accomplished numerically by discretization into a set of simultaneous, complex, algebraic

equations using the rectangular constant elements. The Green's functions of a layered half-space, calculated by the procedure described by LUCO and APSEL [21], have been used in the solution procedure. The matrix $\hat{\mathbf{H}}(\mathbf{x},\omega)$, $\mathbf{x} \in S_C^B$, is obtained from closed-form expressions [5]. The complex-valued impedance matrix of soil $\hat{\mathbf{K}}(\omega)$ in the case of constraints imposed by a rigid rectangular body can be written in the form

$$\hat{\mathbf{K}}(\omega) = \begin{bmatrix} \hat{K}_{H_1H_1} & 0 & 0 & 0 & \hat{K}_{H_1\Theta_2} & 0 \\ 0 & \hat{K}_{H_2H_2} & 0 & \hat{K}_{H_2\Theta_1} & 0 & 0 \\ 0 & 0 & \hat{K}_{VV} & 0 & 0 & 0 \\ 0 & \hat{K}_{\Theta_2H_2} & 0 & \hat{K}_{\Theta_1\Theta_1} & 0 & 0 \\ \hat{K}_{\Theta_2H_1} & 0 & 0 & 0 & \hat{K}_{\Theta_2\Theta_2} & 0 \\ 0 & 0 & 0 & 0 & 0 & \hat{K}_{TT} \end{bmatrix}$$

in which $\hat{K}_{H_iH_i}$, $\hat{K}_{\Theta_i\Theta_i}$, $\hat{K}_{H_i\Theta_j} = \hat{K}_{\Theta_jH_i}$, $\hat{K}_{VV}$ and $\hat{K}_{TT}$ are the horizontal, rocking, coupling, vertical and torsional complex-valued impedance functions, respectively. To give an insight into the dynamic properties of the soil models, the vertical impedance function is widely presented. The function can be written in the form

$$\hat{K}_{VV} = \left(V_S^{(L)}(0)\right)^2 \rho_1 B(k_{vv} + ia_0 c_{vv})$$

where k_{vv} is the normalized vertical stiffness coefficient, c_{vv} is the normalized damping coefficient and $a_0 = \omega B/V_S^{(L)}(0)$ denotes the dimensionless frequency. The non-dimensional stiffness and damping coefficients have been calculated for the following data: $ZE/B = 0$; $L/B = 1$; $\nu_1 = \nu_2 = 0.33$; $\zeta_{1s} = \zeta_{1p} = 0.05$; $\zeta_{2s} = \zeta_{2p} = 0.03$; $\rho_2/\rho_1 = 1.13$; $a_0 \in [0.1, 3]$; $HL/B \in [2, 4]$; $CR = V_S^{(H)}/V_S^{(L)}(0) \in \{1.0, 1.50, 2.0, 2.5, 3.0\}$; number of boundary elements $8 \times 8 = 64$. The assumed values of contrast ratio CR control the jump in the step-step velocity-depth profile and simultaneously, they control the gradient of the linear part of the ramp-step velocity-depth profile. Furthermore, the assumed value of Poisson's ratio is typical for granular soils.

It is seen from Figures 3 and 4 that if the soil resembles a layer overlying a half-space rather than a uniform half-space, the normalized vertical stiffness k_{vv} and damping c_{vv} coefficients exhibit strong dependence on the shape of the shear wave velocity profile in addition to dimensionless frequency a_0. The variations of k_{vv} and c_{vv} with a_0 and HL/B for the first shear wave velocity profile are fluctuating functions and the fluctuations grow with the increase of jump in the piecewise constant profile due to increase of the contrast ratio CR. They are the outcome of resonance phenomena in the pronounced layered medium. On the contrary, the k_{vv} and c_{vv} coefficients are rather smooth functions of the considered parameters for the second, continuous, piecewise linear velocity-depth profile.

a)

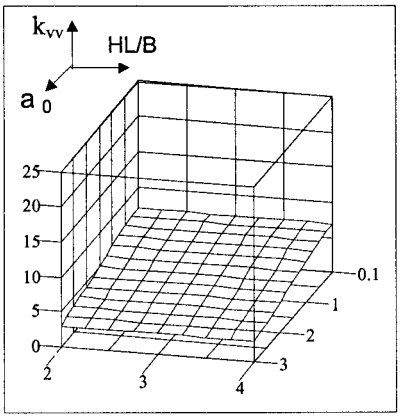
k_{vv}
HL/B
a_0
25
20
15
10
5
0
2
3
4
0.1
1
2
3

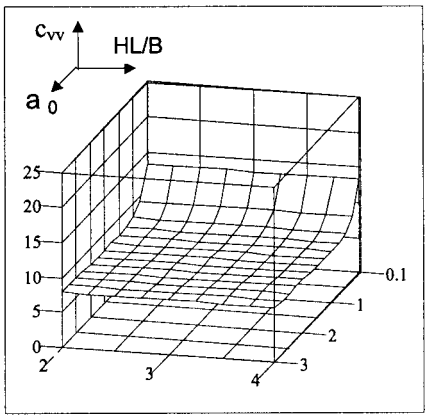
c_{vv}
HL/B
a_0
25
20
15
10
5
0
2
3
4
0.1
1
2
3

b)

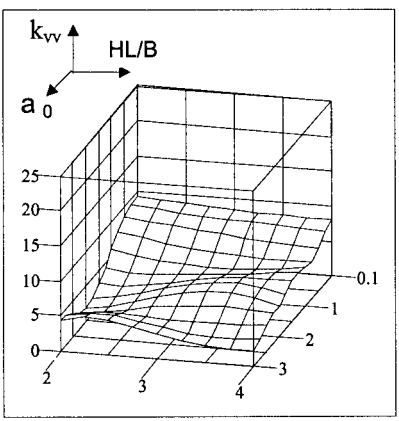
k_{vv}
HL/B
a_0
25
20
15
10
5
0
2
3
4
0.1
1
2
3

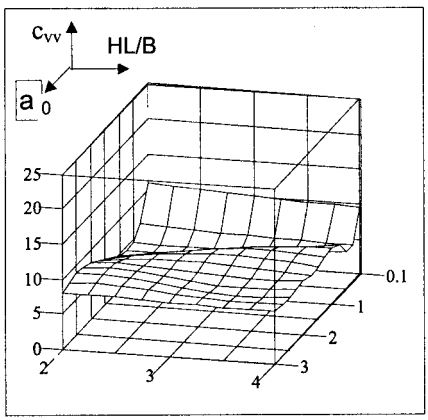
c_{vv}
HL/B
a_0
25
20
15
10
5
0
2
3
4
0.1
1
2
3

c)

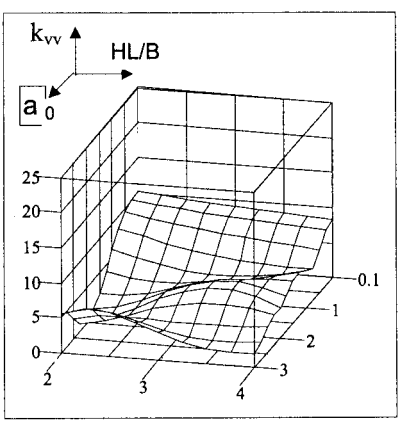
k_{vv}
HL/B
a_0
25
20
15
10
5
0
2
3
4
0.1
1
2
3

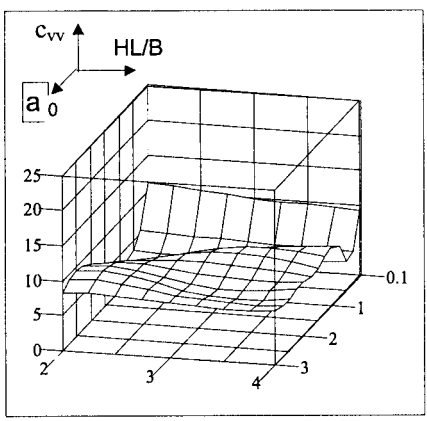
c_{vv}
HL/B
a_0
25
20
15
10
5
0
2
3
4
0.1
1
2
3

[FIG. 3]

[192]

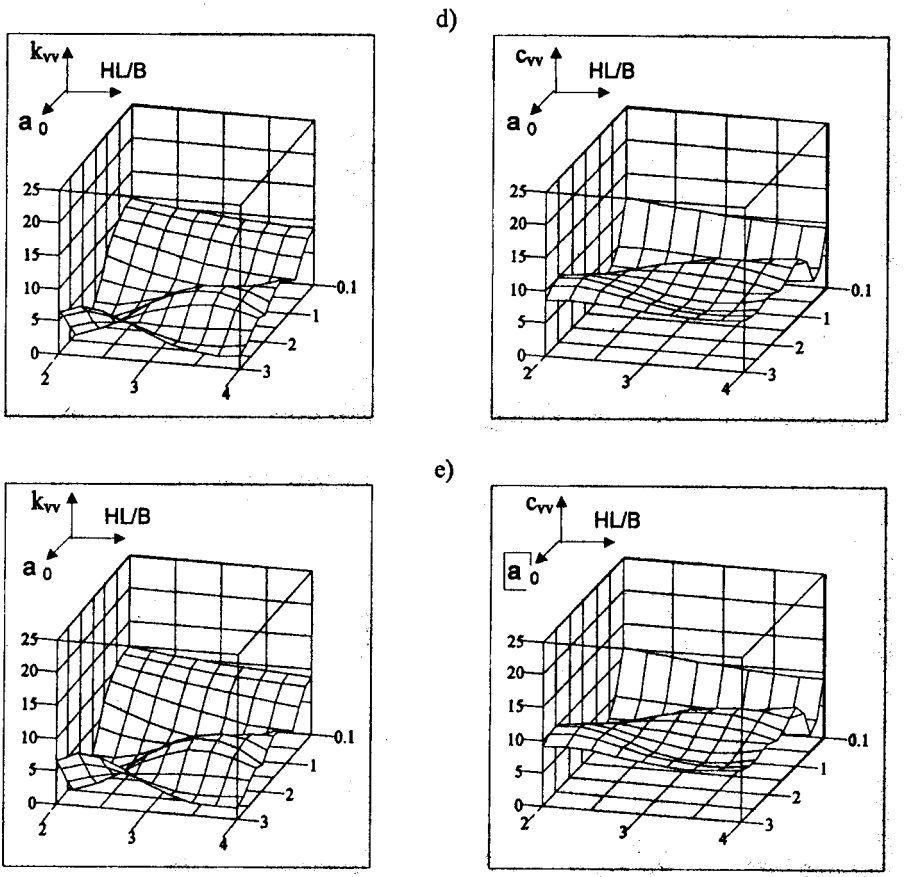

FIG. 3. Normalized vertical stiffness and damping coefficients of a layered soil for shear wave velocity profile (I); a) $CR = 1.0$, b) $CR = 1.50$, c) $CR = 2.0$, d) $CR = 2.5$, e) $CR = 3.0$.

In general, the normalized vertical stiffness coefficient can be greater or lower than the values predicted for a uniform half-space, and the normalized damping coefficient may be considerably lower than that of the homogeneous half-space depending on the shape of the shear velocity profile, the frequency of vibration, the thickness of the layer overlying the half-space and the contrast between the rigidity of the two materials constituting the inhomogeneous supporting medium. Existence of the "zone of influence" (dynamic pressure bulb) is evident from the Figs. 3 and 4. Below the depth of the "bulb", the influence of the properties of the supporting medium on the vertical impedance function at the point of reference on the surface of the supporting medium disappear.

The variations of the dynamic stiffness and damping coefficients presented in Figs. 3 and 4 for the vertical mode of vibration are observed to a larger or smaller degree in all modes of vibration, but details of marked differences are not addressed here.

a)

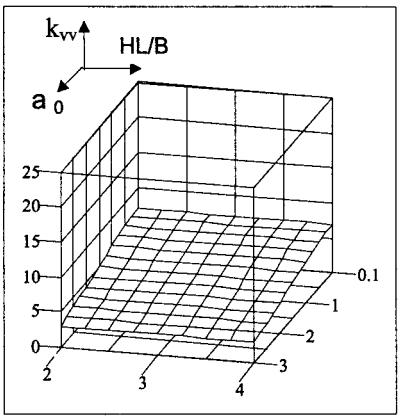
k_{vv}
HL/B
a_0
25
20
15
10
5
0
2
3
4
0.1
1
2
3

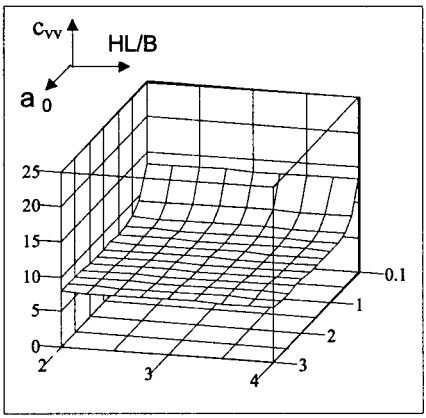
c_{vv}
HL/B
a_0
25
20
15
10
5
0
2
3
4
0.1
1
2
3

b)

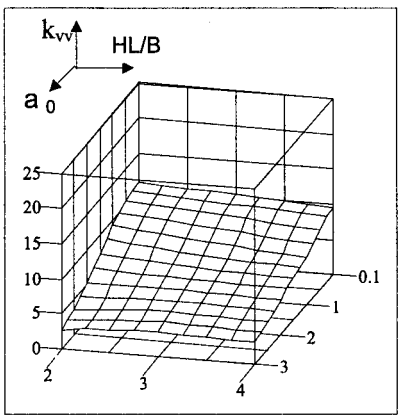
k_{vv}
HL/B
a_0
25
20
15
10
5
0
2
3
4
0.1
1
2
3

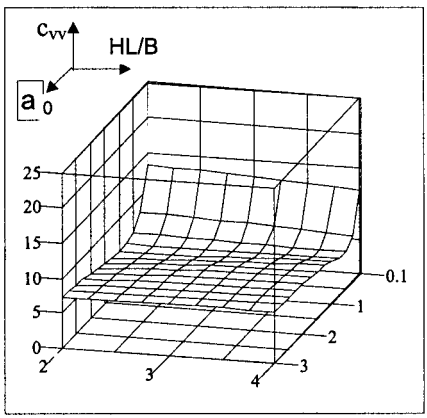
c_{vv}
HL/B
a_0
25
20
15
10
5
0
2
3
4
0.1
1
2
3

c)

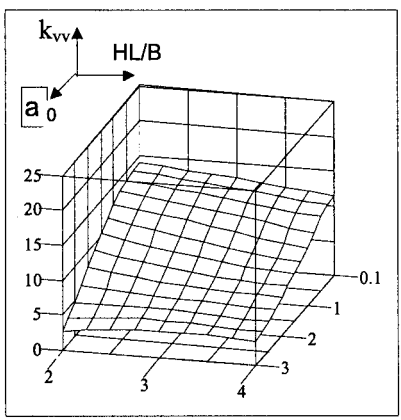
k_{vv}
HL/B
a_0
25
20
15
10
5
0
2
3
4
0.1
1
2
3

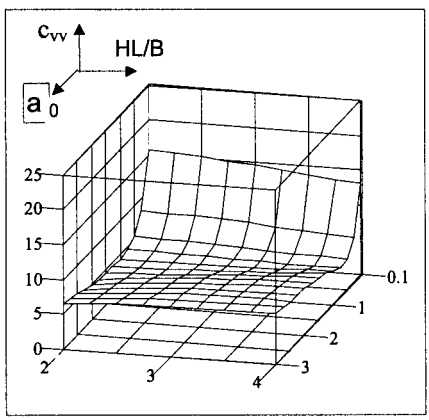
c_{vv}
HL/B
a_0
25
20
15
10
5
0
2
3
4
0.1
1
2
3

[FIG. 4]

[194]

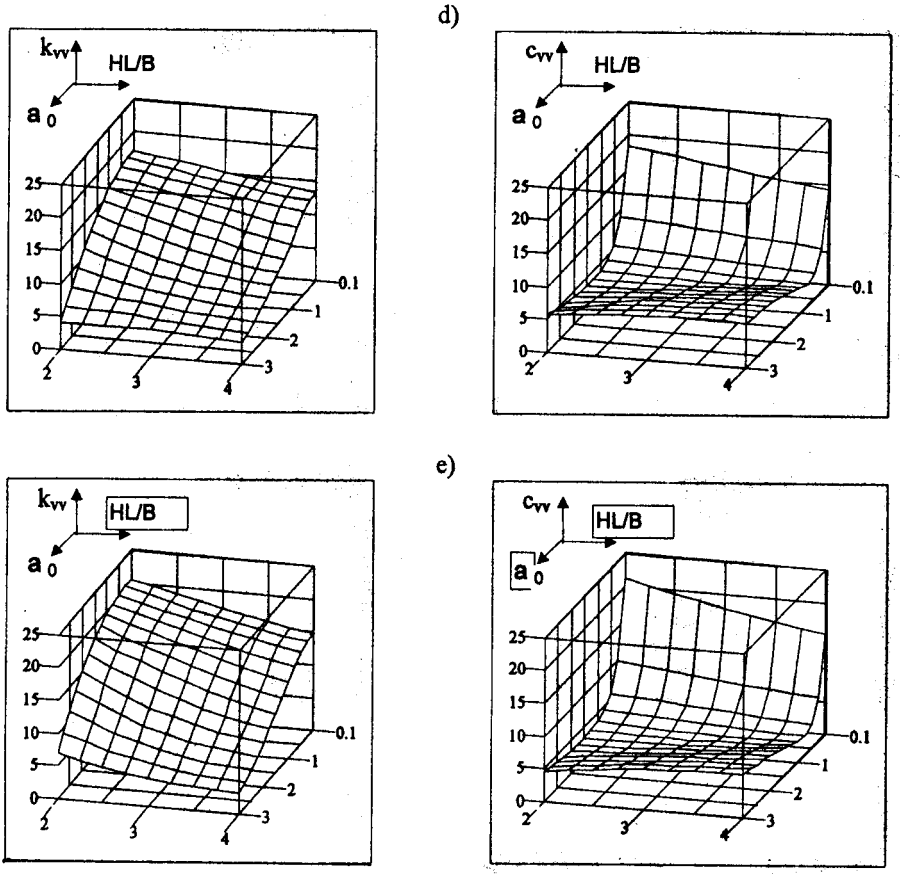

FIG. 4. Normalized vertical stiffness and damping coefficients of a layered soil for shear wave velocity profile (II); a) $CR = 1.0$, b) $CR = 1.50$, c) $CR = 2.0$, d) $CR = 2.5$, e) $CR = 3.0$.

It is well known that at relatively high frequencies, the motion of a rigid massive foundation is controlled by the static stiffnesses of the soil (limit of dynamic stiffnesses at frequency tending to zero). However, at relatively low frequencies encountered in practice the dynamic response of massive rigid foundation reflects the characteristics of both the machine-block inertia and dynamic properties of the supporting medium. It is clear that adequate modelling of the nature of the soil profile is a crucial step in the dynamic analysis of the machine-block-soil system.

To illustrate the effect of the variations of shear wave velocity profile on the minimum mass optimum design of machine foundation block subjected to unbalanced forces of reciprocating machine, the optimal objective function has been determined for several configurations of two particular velocity-depth functions of soil under the block including piecewise constant step-step profile and continuous ramp-step profile and additional effects of backfill.

Two simple types of reciprocating machines mounted on the rectangular concrete blocks are considered. Let a machine with only one cylinder be mounted vertically on a rigid foundation with counterbalancing. Assume that the line of motion of the piston lies along the vertical axis passing through the center of mass of the engine and the foundation. Then the foundation will undergo only vertical vibration. The input data and limiting values of constraints for the optimal design of the foundation to support the vertical single cylinder reciprocating engine are given in Box 3. Values of minimum mass optimum design of block for vertical mode of vibration are presented in Fig. 5.

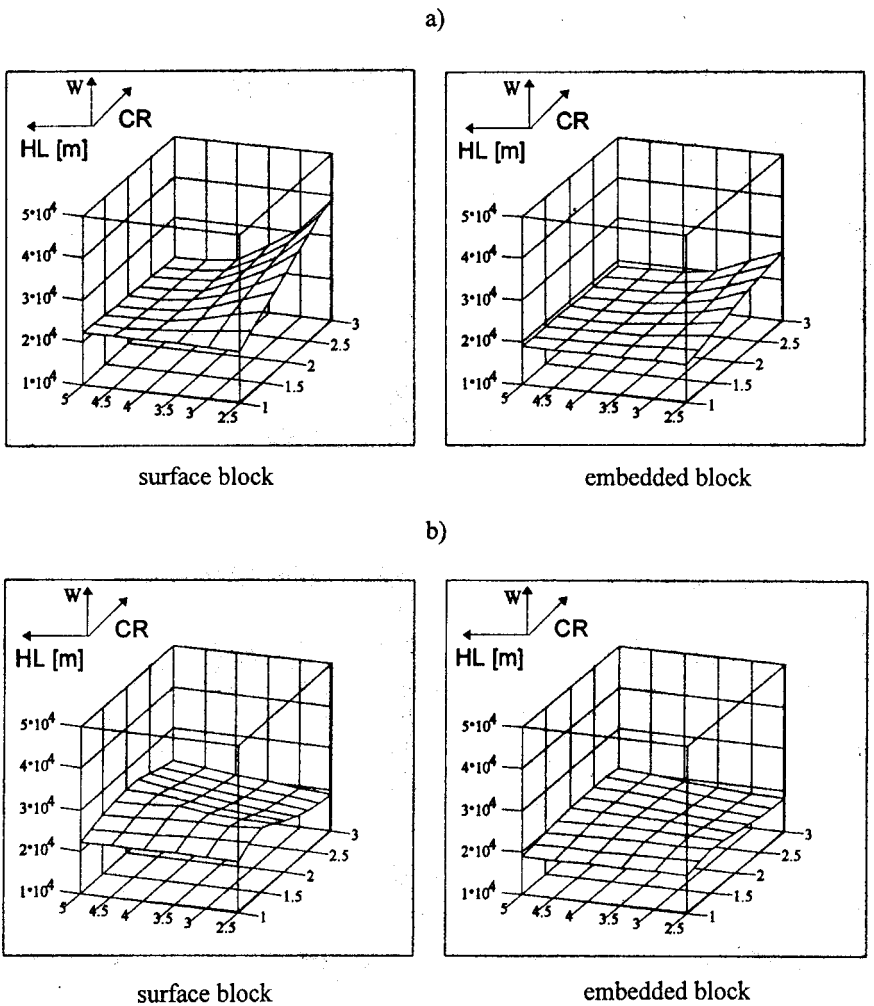

FIG. 5. Optimal objective function W [kg] versus thickness of the layer HL and shear wave velocity ratio CR for vertical vibrations of block; a) shear wave velocity profile (I), b) shear wave velocity profile (II).

Box 3. Input data and limiting values of constraints for vertical vibrations

(1) *machine data*:
mass of machine = 1400.0 kg,
total reciproacting mass M_B = 10.0 kg,
crank length r = 0.08 m,
length of connecting rod 1 = 0.3 lm,
operating speed = 1200 rpm,
$F_z = M_B r\omega^2 \cos\omega t + M_B(r^2\omega^2/l)\cos 2\omega t$,

(2) *block data*:
density of concrete block = 2400.0 kg/m^3,
height HB = 2.0 m,
thickness of base slab HP = 0.5 m,
constant dimensions of top part of block:
YD = 1.5 m, XD = 2.5 m,

(3) *backfill data*:
thickness of backfill layer ZE = 0.0 and 1.0 m,
dynamic shear modulus G_b = 20000.0 kN/m^2,
density ρ_b = 1350.0 kg/m^3,
hysteretic damping constants:
$\zeta_{bs} = \zeta_{bp} = 0.05$,

(4) *soil below the base of block*:
layer
shear modulus
$G_1(0)$ = 40000.0 kN/m^2
Poisson's ratio $\nu_1 = 0.33$,
density ρ_1 = 1650.0 kg/m^3,
hysteretic damping constants
$\zeta_{1s} = \zeta_{1p} = 0.05$,
underlying half-space
Poisson's ratio $\nu_2 = \nu_1$,
density $\rho_2 = 1.13\rho_1$,
hysteretic damping constants
$\zeta_{2s} = \zeta_{2p} = 0.03$,

(5) *limiting values of constraints*:
vertical displacement amplitude
limit $A^{\nu}_{\text{feas}} = 30.0 \times 10^{-6}$ m,
stresses in the soil limit
σ_{feas} = 150.0 kN/m^2,
size limits: 2.5 m $\leqslant D_1 \leqslant$ 5.5 m
$1.5 \leqslant D_2 \leqslant 4.5$ m.

In the next example, a single cylinder reciprocating engine is mounted horizontally and symmetrically on the rectangular rigid block and counterweights are not installed. It means that the centre of the crank lies vertically above the mass centre of the machine-block system and the plane of crank rotation lies in the plane of symmetry of the system. In this case the foundation will undergo vertical and coupled rocking and sliding oscillations. The input data and limiting values of constraints for optimal design of the foundation to support the horizontal single cylinder reciprocating engine are given in Box 4. The results of the optimization process are shown in Fig. 6.

An inspection of the Figure 5 indicates that for vertically vibrating block resting on a layered medium with discontinuous step-step velocity-depth function, the minimum optimal mass increases with the increase of jump between two parts of the profile but decreases with increasing values of the thickness of the layer overlying the half-space. The global maximum of the objective function (the "worst case") exists for the contrast ratio $CR = 3$ and the layer thickness HL = 2.5 m. Then, the existence of very stiff material at a relatively shallow depth may

Box 4. Input data and limiting values of constraints for coupled vibrations

(1) *machine data*:
mass of machine = 1500.0 kg,
mass moment of inertia of the machine about an axis passing through its centre of mass = 2500 kgm^2,
total rotating mass $M_A = 7.25$ kg,
total mass due to piston and crank rod $M_B = 13.15$ kg,
length of connecting rod 1 = 0.45 m,
operating speed = 600 rpm ($\omega = 20\pi$ rad/s),
height of machine CG above the top of the block = 0.3 m
unbalanced forces (vertical and horizontal):
$F_v = M_A r\omega^2 \sin\omega t$,
$F_h = (M_A + M_B) r\omega^2 \cos\omega t + M_B(r^2\omega^2/l)\cos 2\omega t$,

(2) *block data*:
density of concrete block = 2400.0 kg/m^3,
height $HB = 1.5$ m,
thickness of base slab $HP = 0.5$ m,
constant dimensions of top part of block:
$YD = 1.5$ m, $XD = 1.5$ m,

(3) *backfill data*:
thickness of backfill layer $ZE = 0.0$ and 1.0 m,
dynamic shear modulus $G_b = 30000.0$ kN/m^2,
density $\rho_b = 1350.0$ kg/m^3,
Poisson's ratio = 0.25,
hysteretic damping constants:
$\zeta_{bs} = \zeta_{bp} = 0.05$,

(4) *soil below the base of block*:
layer
shear modulus $G_1(0) = 60000.0$ kN/m^2
Poisson's ratio $\nu_1 = 0.33$,
density $\rho_1 = 1650.0$ kg/m^3,
hysteretic damping constants $\zeta_{1s} = \zeta_{1p} = 0.05$,
underlying half-space
Poisson's ratio $\nu_2 = \nu_1$,
density $\rho_2 = 1.13\rho_1$,
hysteretic damping constants $\zeta_{2s} = \zeta_{2p} = 0.03$,

(5) *limiting values of constraints*:
total vertical displacement amplitude limit $A^v_{\text{feas}} = 60.0 \times 10^{-6}$ m,
total horizontal displacement amplitude limit $A^h_{\text{feas}} = 90.0 \times 10^{-6}$ m,
stress in the soil limit $\sigma_{\text{feas}} = 150.0$ kN/m^2,
size limits: 1.5 m $\leqslant D_1 \leqslant$ 3.5 m, 1.5 m $\leqslant D_2 \leqslant$ 3.5 m.

drastically influence the optimal design. In the case of continuous ramp-step velocity-depth profile the optimum mass trends displayed a different pattern. Small increase is observed for relatively low values of contrast ratio CR depending on the layer thickness HL, when the effect of the reduction of radiation damping is greater than the effect of increase of the stiffness. However, the increase of gradient of the linear part of the velocity-depth function increases the vertical stiffness leading finally to the reduction of optimal mass that reaches its global minimum at the same point as the global maximum for the first velocity-depth profile. If the block is surrounded by backfill, the values of total stiffness and damping coefficients of the supporting medium substantially increase. It reduces the values of the minimum optimal mass and the sensitivity with respect to variations in the velocity-depth profiles.

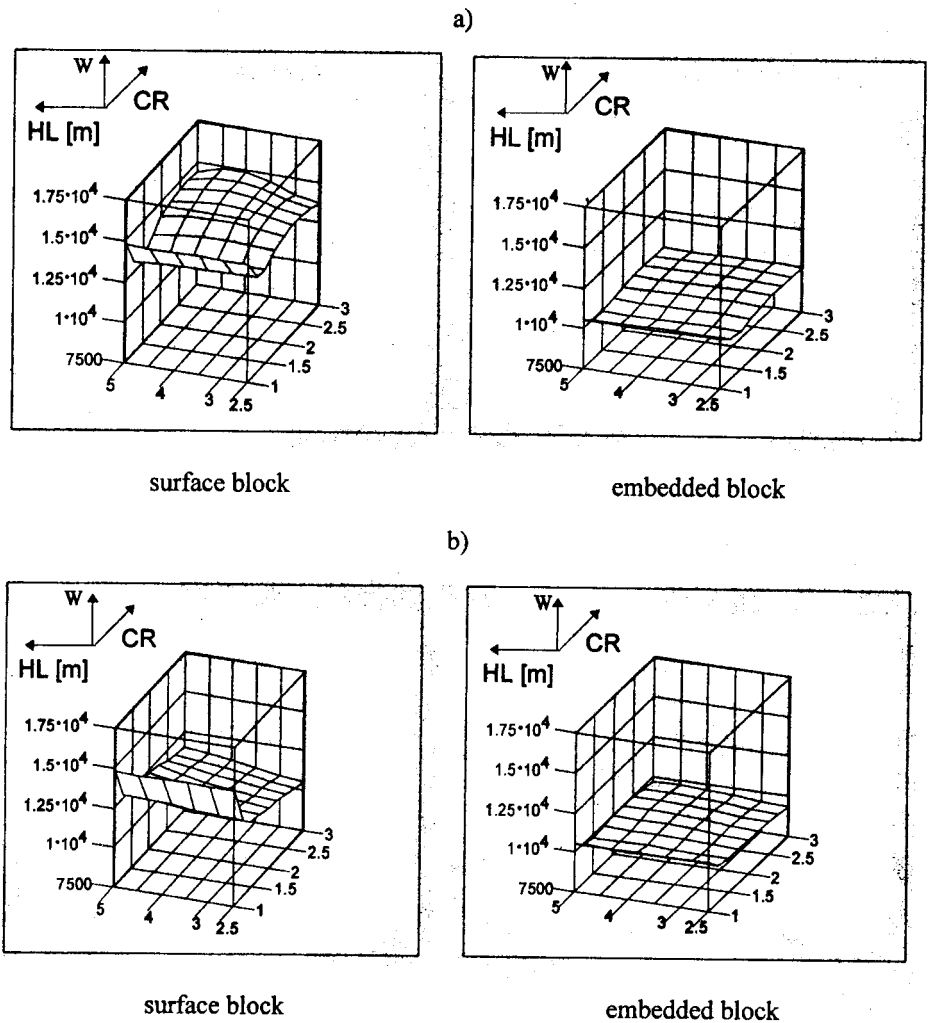

FIG. 6. Optimal objective function W [kg] versus thickness of the layer HL and shear wave velocity ratio CR for coupled vibrations of block; a) shear wave velocity profile (I), b) shear wave velocity profile (II).

In the case of complex dynamic loading of block resting on a pronounced layered medium (first velocity-depth profile), the minimum optimal mass displays rather small variations, its decreasing or increasing depend on the values of the layer thickness HL and the contrast ratio CR. For the second velocity-depth profile, the minimum optimal mass decreases monotonically with increasing values of contrast ratio CR but increases monotonically with increasing values of the thickness of the layer HL. It reaches the global minimum for the contrast ratio $CR = 3$ and the layer thickness $HL = 2.5$ m. Figure 6 serves also to illustrate the main effects of the embedment of the block on minimum optimal mass. Si-

gnificant reductions of the minimum optimal mass are observed for all considered combinations of velocity-depth profiles. Also, it is not sensitive to changes in the values of parameters HL and CR. It is seen from the Figs. 5 and 6 that the effect of embedding of the block is greater for the coupled mode of vibration than for the vertical mode of vibration, agreeing qualitatively with physical intuition.

6. Concluding remarks

Soil-block interaction has a considerable influence on the dynamic response of massive rigid machine foundation supported by soil deposits. Computational difficulties are primary due to the three-dimensional, semi-infinite nature of the soil medium and variation of the soil properties with depth. Often it is not easy to correlate the variations as found by measurements to those of idealized systems. The adopted velocity-depth profiles in the form of piecewise continuous step-step function and continuous ramp-step function make possible a realistic and economical assessment of sensitivity of minimum mass optimal design with respect to changes in preassigned parameters defining depth-dependent properties of strongly as well as weakly layered media with bounded nonhomogeneity.

The sensitivity analysis of minimum mass optimum design of block based on the reoptimization displays trends that depend on the form of velocity-depth profile, the mode of vibration and the depth of embedment.

The presented results can be used to predict revised optimum designs, associated with specified changes of parameters defining the velocity-depth profile. Furthermore, they provide a useful basis for clarifying the role of uncertainties in modelling of the dynamic properties of the semi-infinite soil deposits.

Acknowledgement

The present work is partially supported by a grant No. 7 T07E 029 13 from the Committee for Scientific Research (KBN).

References

1. J. Lipiński, *Foundations for machines* [in Polish], Arkady, Warszawa 1985.
2. P. J. Moore [Ed.], *Analysis and design of foundations for vibrations*, A. A. Balkema, Rotterdam 1985.
3. G. Gazetas, *Analysis of machine foundation vibrations: state-of-the-art*, Soil Dyn. Earthquake Engng., **3**, 1, 2–42, 1983.
4. J. P. Wolf, *Dynamic soil-structure interaction*, Prentice-Hall, Englewood Cliffs, N.J. 1985.

5. Z. SIENKIEWICZ, *Forced vibrations of rectangular foundations embedded in a half-space*, Archives of Civil Engng, **38**, 35–58, 1996.

6. K. DEMS and W. GUTKOWSKI, *2D shape optimization with static and dynamic constraints*, Structural Optimization, **15**, 3/4, 201–207, 1998.

7. B. ESPING, *Design optimization as on engineering tool*, Structural Optimization, **10**, 3/4, 137–152, 1995.

8. Z. SIENKIEWICZ and B. WILCZYŃSKI, *Minimum-weight design of machine foundation under vertical load*, ASCE J. of Engng. Mech., **119**, 1781–1797, 1993.

9. Z. SIENKIEWICZ and B. WILCZYŃSKI, *Shape optimization of a dynamically loaded machine foundation coupled to a semi-infinite inelastic medium*, Structural Optimization, **12**, 29–34, 1996.

10. Z. SIENKIEWICZ and B. WILCZYŃSKI, *Shape optimization of a dynamically loaded machine foundation coupled to layered subsoil*, W. Gutkowski and Z. Mróz [Eds.], Proc. Second World Congress of Structural and Multidisciplinary Optimization, WCSMO-2, Zakopane, May, 26–30, Poland, 637–642, 1997.

11. Z. SIENKIEWICZ and B. WILCZYŃSKI, *Weight minimization of dynamically loaded 3-D foundation on layered medium*, S. Hernandez and C.A. Brebbia [Eds.], Computer-Aided Optimum Design of Structures V, Computational Mechanics Publications, Southampton, 131–140, 1997.

12. L.A. SCHMIT and K.J. CHANG, *Optimum design sensitivity based on appromation concepts and dual methods*, Int. J. Numer. Meth. in Engng., **20**, 39–75, 1984.

13. Y. HAN, *Coupled vibration of embedded foundation*, ASCE J. of Geotechnical Engng, **115**, 1227–1238, 1989.

14. A.C. ERINGEN, E.S. SUHUBI, *Elastodynamics*, Vol. 2-linear theory, Academic Press, New York 1975.

15. M. NOVAK, T. NOGAMI, F. ABOUL-ELLA, *Dynamics soil reactions for plane strain case*, ASCE J. of Engng. Mech. Div., **104**, 953–959, 1978.

16. A. BORKOWSKI, K. DEMS, W. GUTKOWSKI and Z. MRÓZ, *Optimization methods*, [In:] M. Kleiber [Ed.] Computer methods of solid mechanics, [in Polish] PWN, Warszawa 1995, 519–645.

17. J-F. M. BARTHELEMY and R.T. HAFTKA, *Approximation concepts for optimum structural design-a-review*, Structural Optimization, **5**, 129–144, 1993.

18. U. KIRSCH, *Effective move limits for approximate structural optimization*, ASCE J. of Structural Engng., **123**, 210–217, 1997.

19. K. SCHITTKOWSKI, C. ZILLOBER and R. ZOTEMANTEL, *Numerical comparision of nonlinear programming algorithms for structural optimization*, Structural Optimization, **7**, 1–19, 1994.

20. T.-Y. CHEN, *Calculation of the move limits for the sequential linear programming method*, Int. J. Num. Meth. Engng., **36**, 2661–2679, 1993.

21. J.E. LUCO and R.J. APSEL, *On the Green's functions for layered half-space: part* I, Bull. Seism. Soc. Am., **73**, 909–924, 1983.

Received Dezember 1, 1998.